Inorg. Chem. **2007**, *46*, 6661–6667

Study of $Ba_3M^{II}M^{IV}WO_9$ (M^{II} = Ca, Zn; M^{IV} = Ti, Zr) Perovskite Oxides: Competition between 3C and 6H Perovskite Structures

Rohini Mani, P. Selvamani, Joby E. Joy, and J. Gopalakrishnan*

Solid State and Structural Chemistry Unit, Indian Institute of Science, Bangalore 560 012, India

Tapas Kumar Mandal

Department of Chemistry and Chemical Biology, Rutgers, The State University of New Jersey, Piscataway, New Jersey 08854

Received April 23, 2007

We describe an investigation of $Ba_3M^{II}M^{IV}WO_9$ oxides for M^{II} = Ca, Zn, and other divalent metals and M^{IV} = Ti, Zr. In general, a 1:2-ordered 6H (hexagonal, $P6_3/mmc$) perovskite structure is stabilized at high temperatures (1300 °C) for all of the $Ba_3M^{II}TiWO_9$ oxides investigated. An intermediate phase possessing a partially ordered 1:1 double perovskite (3C) structure with the cation distribution, $Ba_2(Zn_{2/3}Ti_{1/3})(W_{2/3}Ti_{1/3})O_6$, is obtained at 1200 °C for $Ba_3ZnTiWO_9$. Sr substitution for Ba in the latter stabilizes the cubic 3C structure instead of the 6H structure. A metastable $Ba_3CaZrWO_9$ that adopts the 3C (cubic, $Fm\bar{3}m$) structure has also been synthesized by a low-temperature metathesis route. Besides yielding several new perovskite oxides that may be useful as dielectric ceramics, the present investigation provides new insights into the complex interplay of crystal chemistry (tolerance factor) and chemical bonding (anion polarization and d^0-induced distortion of metal–oxygen octahedra) in the stabilization of 6H versus 3C perovskite structures for the $Ba_3M^{II}M^{IV}WO_9$ series.

Introduction

Among the several ordered variants of the perovskite ($CaTiO_3 \equiv AMO_3$) structure,[1] M-site cation-ordered triple perovskites of the formula $A_3MM'_2O_9$ are a special family that has received considerable attention in recent times,[2−6] in view of the structural diversity and technologically important material properties exhibited by members of this family. $Ba_3ZnTa_2O_9$, a prototypical member of this family, is a dielectric ceramic that finds application in mobile telecommunication networks/devices.[7,8] Two different, but related, structures are common for these oxides.[1] One is the so-called 3C perovskite structure consisting of an all-cubic (ccc) stacking of closed-packed AO_3 sheets, wherein the M atoms are ordered at the octahedral sites in the sequence ...M−M′−M′−M... along the $\langle 111\rangle_{perovskite}$ direction, giving a trigonal ($P\bar{3}m1$) symmetry for the ideal case (Figure 1a). $Ba_3SrTa_2O_9$ and $Ba_3ZnTa_2O_9$ are typical examples of this structure.[9−11] Another competitive structure for this composition is the so-called 6H structure (hexagonal, $P6_3/mmc$), wherein the AO_3 sheets stack in a mixed cubic−cubic−hexagonal (cchcch) sequence and the M and M′ atoms are ordered in all-oxygen octahedral sites (Figure 1b). A significant difference between the two structures is that, while the $MO_6/M'O_6$ octahedra are exclusively connected through corners in the 3C structure, two of the $M'O_6$ octahedra share a common face, forming M'_2O_9 dimers that are connected to the third MO_6 octahedron through corners in the 6H

* To whom correspondence should be addressed. E-mail: gopal@sscu.iisc.ernet.in. Tel: +91 80 2293 2537. Fax: +91 80 2360 1310.

(1) Mitchell, R. H. *Perovskites: Modern and Ancient*; Almaz Press: Thunder Bay, Canada, 2002.
(2) Rijssenbeek, J. T.; Saito, T.; Malo, S.; Azuma, M.; Takano, M.; Poeppelmeier, K. R. *J. Am. Chem. Soc*. **2005**, *127*, 675.
(3) Bieringer, M.; Moussa, S. M.; Noailles, L. D.; Burrows, A.; Kiely, C. J.; Rosseinsky, M. J.; Ibberson, R. M. *Chem. Mater*. **2003**, *15*, 586.
(4) Lufaso, M. W. *Chem. Mater*. **2004**, *16*, 2148.
(5) Doi, Y.; Wakeshima, M.; Hinatsu, Y.; Tobo, A.; Ohoyama, K.; Yamaguchi, Y. *J. Mater. Chem.* **2001**, *11*, 3135.
(6) Stitzer, K. E.; Smith, M. D.; Gemmill, W. R.; zur Loye, H.-C. *J. Am. Chem. Soc*. **2002**, *124*, 13877.
(7) Vanderah, T. A. *Science* **2002**, *298*, 1182.
(8) Moussa, S. M.; Ibberson, R. M.; Bieringer, M.; Fitch, A. N.; Rosseinsky, M. J. *Chem. Mater*. **2003**, *15*, 2527.
(9) Galasso, F.; Barrante, J. R.; Katz, L. *J. Am. Chem. Soc*. **1961**, *83*, 2830.
(10) Jacobson, A. J.; Collins, B. M.; Fender, B. E. F. *Acta Crystallogr., Sect. B* **1976**, *32*, 1083.
(11) Zandbergen, H. W.; Ijdo, D. J. W. *Acta Crystallogr., Sect. C* **1983**, *39*, 829.

10.1021/ic7007655 CCC: $37.00
Published on Web 07/14/2007

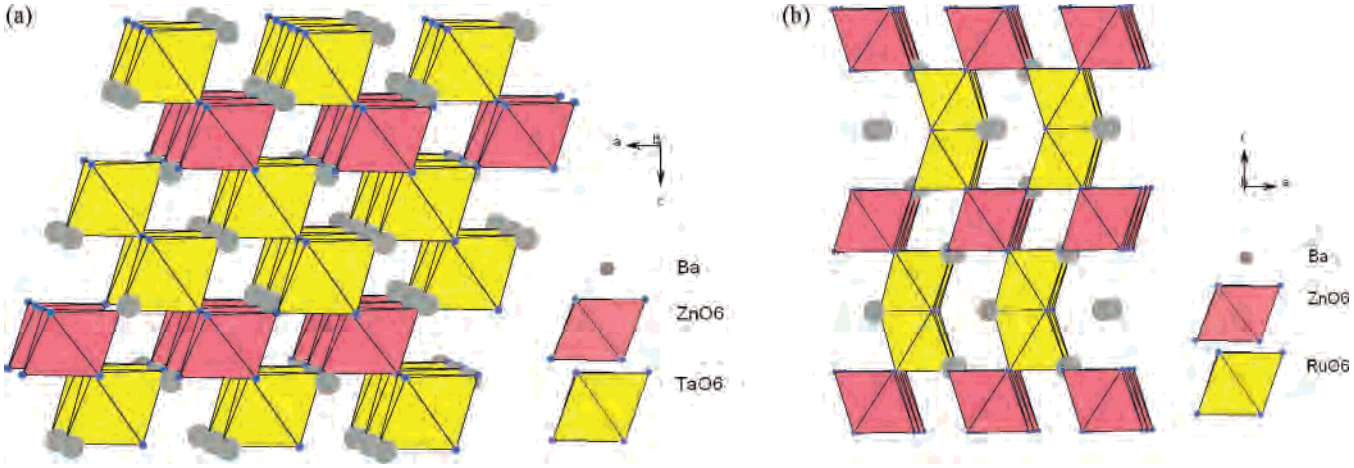

Figure 1. Crystal structures of $Ba_3MM'_2O_9$: (a) 3C structure of $Ba_3ZnTa_2O_9$; (b) 6H structure of $Ba_3ZnRu_2O_9$.

structure. $Ba_3MRu_2O_9$ (M = 3d or lanthanide metal) are representative examples of oxides adopting this structure.[5,12] It appears that, in general, $Ba_3MM'_2O_9$ oxides adopt the 3C structure for M′ d^0 atoms and the 6H structure for M′ d^n atoms, although there are exceptions.[2,13]

The present work is motivated by two objectives : the primary objective is to find new analogues of $Ba_3ZnTa_2O_9$ that would avoid the use of costly Ta.[7] Toward this, we chose the $2Ta^V \rightarrow Ti^{IV}/Zr^{IV} + W^{VI}$ substitution strategy. The second, more general, objective is to understand and rationalize the crystal-chemical factors that control the formation of 3C versus 6H structures for this series of oxides. Accordingly, we investigated the formation and structures of $Ba_3M^{II}M^{IV}WO_9$ oxides for M^{II} = Ca, Zn, or other divalent metal atoms and M^{IV} = Ti or Zr. We have also investigated partial substitution of Sr for Ba in one of the members, $Ba_3ZnTiWO_9$, to probe the role of the tolerance factor. We could prepare ordered perovskite oxides in several cases. Our investigations, which are described herein, shed new light on the stability of the two structures for the $Ba_3M^{II}M^{IV}WO_9$ oxides in general, besides providing M-site ordered perovskite oxides that could be important dielectric ceramic materials.

Experimental Section

Synthesis. Members of the Ba_3MTiWO_9 series for M = Ca, Zn (and other divalent metals such as Mg, Co, and Ni) were synthesized by conventional solid-state reactions of the starting materials ($BaCO_3$, $MC_2O_4{\cdot}2H_2O$, TiO_2, and WO_3) taken in stoichiometric proportion, at elevated temperatures (up to 1300 °C). Oxides of the series $Ba_{3-x}Sr_xZnTiWO_9$ (x = 0, 0.64, and 0.65) were also synthesized similarly, covering the sample pellets by powders of the same composition (to minimize the Zn volatilization at high temperatures).[3] $Ba_3CaZrWO_9$ was synthesized by a new one-pot Li-precursor route developed by us.[14] For this purpose, a stoichiometric mixture of Li_2CO_3, $CaCO_3$, ZrO_2 (dried at 550 °C), WO_3, and $BaCl_2$ were reacted at 800 °C. Product formation occurred in the reaction

$$3Li_2CO_3 + CaCO_3 + ZrO_2 + WO_3 + 3BaCl_2 \rightarrow Ba_3CaZrWO_9 + 6LiCl + 4CO_2 \quad (1)$$

Table 1. Synthesis Conditions, Structure Type, and Lattice Parameters of $Ba_3M^{II}M^{IV}WO_9$ Oxides

composition	t^a	synthesis conditions[b] (°C/h)	structure and lattice param
$Ba_3CaTiWO_9$	0.997	300/3, 1200/24, 1300/24	6H: hexagonal a = 5.9246(2) Å c = 14.6761(5) Å
$Ba_3MgTiWO_9$	1.042	300/3, 1200/24, 1300/48 + 24	6H: hexagonal a = 5.783(1) Å c = 14.103(9) Å
$Ba_3CoTiWO_9$	1.055	300/3, 1300/24	6H: hexagonal a = 5.760(5) Å c = 14.142(5) Å
$Ba_3NiTiWO_9$	1.047	300/3, 1300/24	6H: hexagonal a = 5.751(1) Å c = 14.007(8) Å
$Ba_3ZnTiWO_9$	1.039	300/3, 1200/24, 1300/24	6H: hexagonal a = 5.8030 (1) Å c = 14.1696(2) Å
$Ba_3ZnTiWO_9$	1.039	300/3, 1200/24	3C: monoclinic a = 5.712(5) Å b = 5.650(3) Å c = 8.094(4) Å β = 90.31(6)°
$Ba_{2.36}Sr_{0.64}ZnTiWO_9$	1.027	300/3, 1200/24, 1300/24	3C: cubic a = 8.082(2)
$Ba_{2.35}Sr_{0.65}ZnTiWO_9$	1.026	300/3, 1200/24, 1300/24	3C: cubic a = 8.032(3) Å
$Ba_3CaZrWO_9$	0.979	800/24	3C: cubic a = 8.3801(1) Å

[a] Goldschmidt tolerance factor $t = (r_A + r_O)/[\sqrt{2}(r_M + r_O)]$ where r_A and r_M are the ionic radii of A-site cations (12-coordination) and M-site cations (6-coordination), respectively; r_O is the radius of the oxide ion (1.40 Å). [b] All of the oxides except $Ba_3CaZrWO_9$ were prepared by a conventional solid-state reaction of the constituents at elevated temperatures. $Ba_3CaZrWO_9$ was prepared by a one-pot metathesis route (see the Experimental Section for details).

and the product was washed with distilled water and dried at 120 °C. The chemical composition and synthesis conditions, together with other structural parameters for the compounds synthesized, are summarized in Table 1.

Structural Characterization. The solid products were characterized by scanning electron microscopy (SEM), energy-dispersive X-ray (EDX) analysis, and powder X-ray diffraction (XRD). A JEOL JSM 5600 LV microscope fitted with a Link/ISIS system from Oxford Instruments was used to carry out SEM and EDX

(12) Lightfoot, P.; Battle, P. D. *J. Solid State Chem.* **1990**, *89*, 174.
(13) Blasse, G. *J. Inorg. Nucl. Chem.* **1965**, *27*, 993.

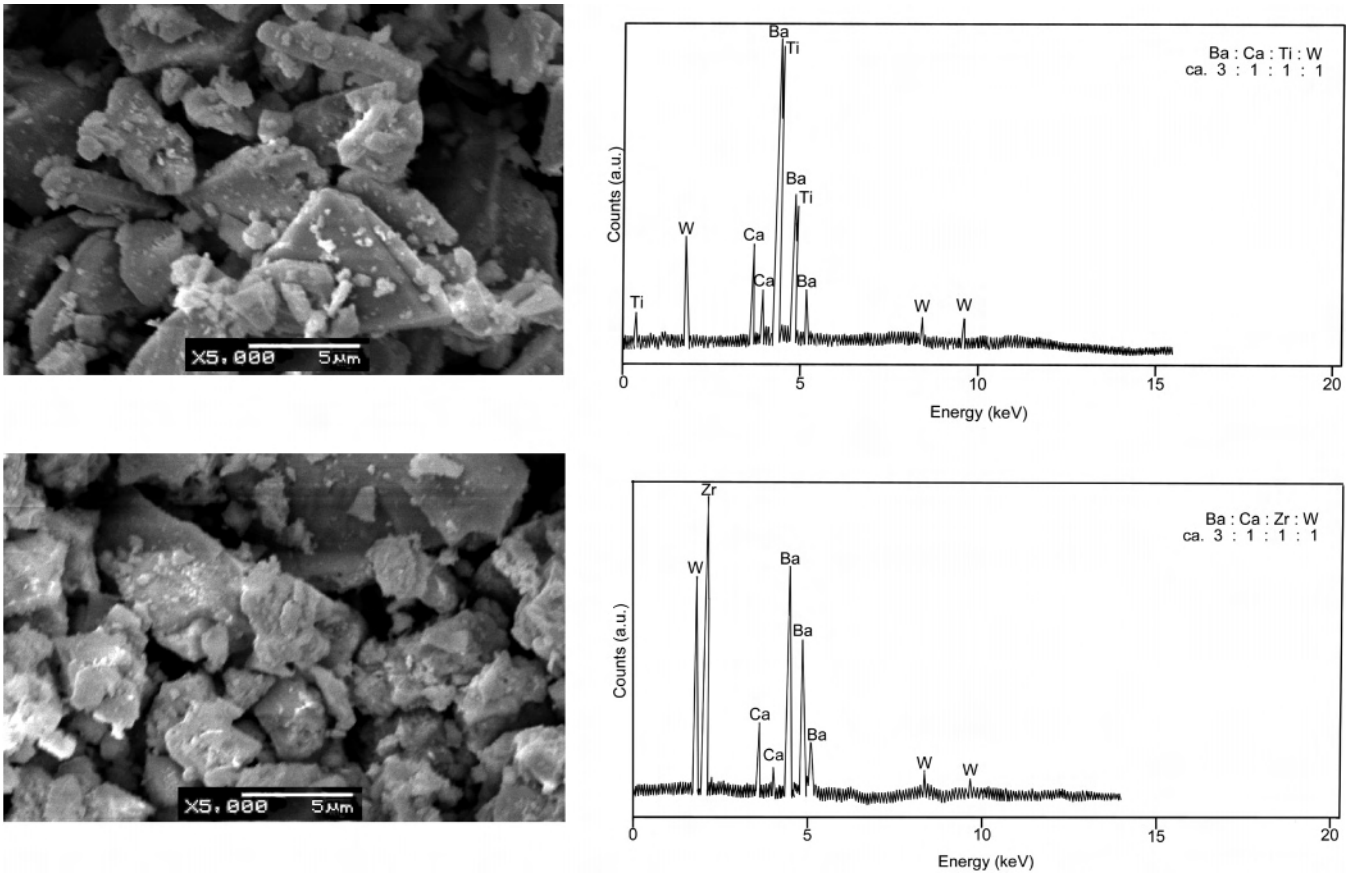

Figure 2. SEM images of $Ba_3CaTiWO_9$ (top) and $Ba_3CaZrWO_9$ (bottom). The corresponding EDX data are shown in the right-side panels. The average metal atom ratios are indicated.

analyses. A Philips X'Pert diffractometer (Ni-filtered Cu Kα radiation) was employed to record powder XRD patterns. Lattice parameters were obtained by least-squares refinement of powder XRD data by the program *PROSZKI*.[15] Powder XRD patterns were also simulated by the program *POWDERCELL*.[16]

Rietveld refinement of the crystal structures in selected cases was carried out by the *FULLPROF* program.[17] For structure refinements, the XRD data were collected in the 2θ range of 3−100° with a step size of 0.02° and a step time of 9 s with the Philips X'Pert diffractometer (Cu Kα radiation). The patterns were typically refined for the background, zero, scale factor, pseudo-Voigt profile function (*U*, *V*, *W*, and *X*), lattice parameters, atomic parameters, and isothermal temperature factors (B_{iso}).

Results and Discussion

We investigated the formation of $Ba_3M^{II}M^{IV}WO_9$ oxides for several M^{II} (including Ca and Zn) and M^{IV} = Ti or Zr. SEM and EDX analyses of the products showed the formation of single-phase materials with the expected metal atom ratios (within an experimental error of 2%); typically, particle sizes were in the micron range with clean grain boundaries (Figure 2). Powder XRD patterns (Figure 3) revealed that the major phase was a 1:2 M-site ordered perovskite oxide with the hexagonal (6H) structure. However, minor impurity phases corresponding to $BaWO_4$ and a 1:1 M-site ordered cubic (3C) perovskite were seen in several instances. We could obtain a single-phase material without a discernible impurity for $Ba_3CaTiWO_9$ (Figure 3a). We have refined the structure of this phase from powder XRD data. Refinement results (Figure 4 and Table 2) show that the material possesses the 6H hexagonal ($P6_3/mmc$) perovskite

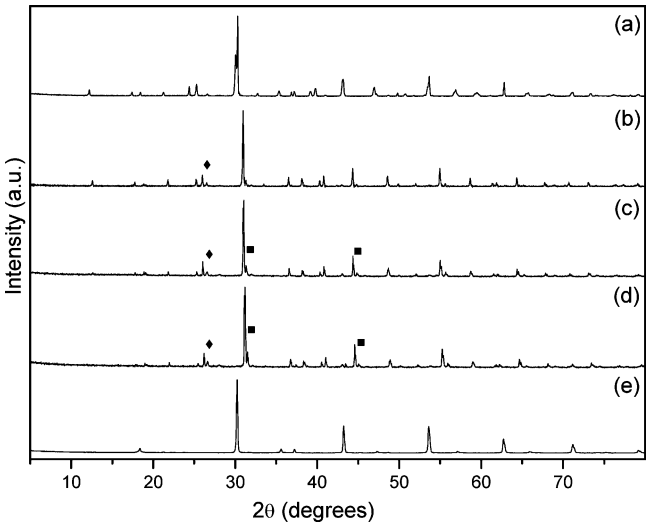

Figure 3. Powder XRD patterns of Ba_3MTiWO_9. M = (a) Ca, (b) Mg, (c) Co, and (d) Ni. Impurity phase reflections [$BaWO_4$ (◆) and 3C (■) phase] are marked. In part e, the XRD pattern of $Ba_3CaZrWO_9$ is shown.

(14) Mani, R.; Bhuvanesh, N. S. P.; Ramanujachary, K. V.; Green, W.; Lofland, S. E.; Gopalakrishnan, J. *J. Mater. Chem.* **2007**, *16*, 1589.
(15) Lasocha, W.; Lewinski, K. *J. Appl. Crystallogr.* **1994**, *27*, 437.
(16) Kraus, W.; Nolze, G. *J. Appl. Crystallogr.* **1996**, *29*, 301.
(17) Rodriguez-Carvajal, J. Multi-Pattern Rietveld Refinement Program *FullProf*.2k, version 3.30, June 2005-LLB.

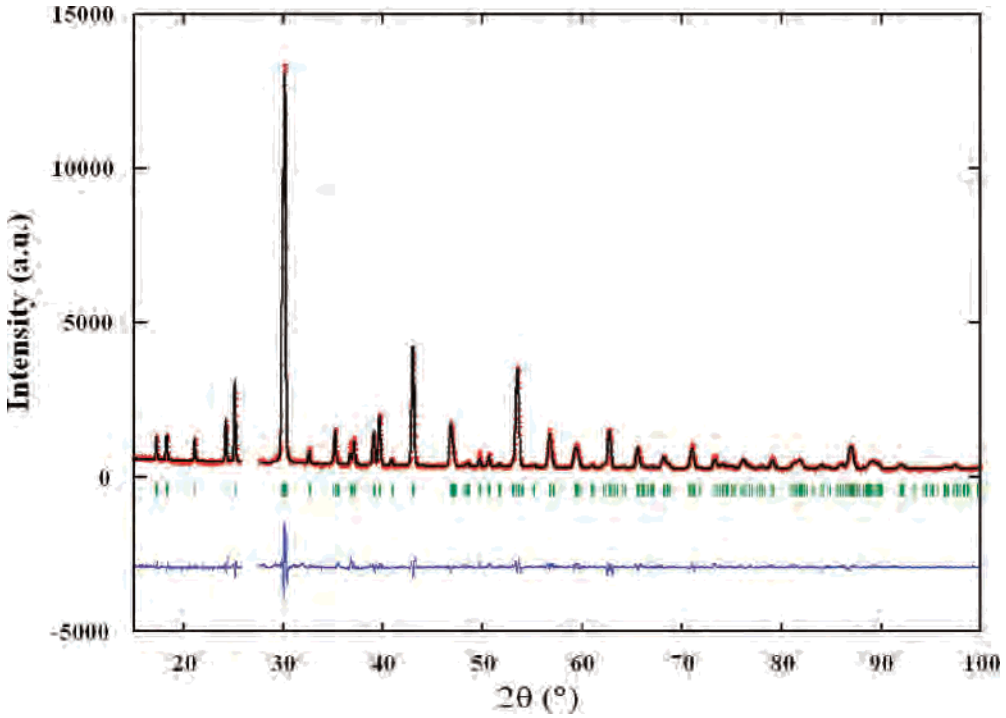

Figure 4. Rietveld refinement of the structure of $Ba_3CaTiWO_9$ (6H) from powder XRD data. Observed (●), calculated (—), and difference (bottom) profiles are shown. The vertical bars indicate positions of the Bragg reflections. The 2θ region (25.93−27.58°) corresponding to $BaWO_4$ impurity reflection is excluded from the refinement.

Table 2. Crystallographic Data for a $Ba_3CaTiWO_9$ (6H) Perovskite, Together with Selected Bond Lengths and Bond Valence Sums[a]

atom	site	*x*	*y*	*z*	*B* (Å^2)	occupancy
Ba1	2b	0.0	0.0	0.25	0.2(1)	1
Ba2	4f	$^1/_3$	$^2/_3$	0.8980(1)	1.0(1)	1
Ca	2a	0.0	0.0	0.0	0.3(1)	1
Ti	4f	$^1/_3$	$^2/_3$	0.1539(1)	0.3(1)	0.5
W	4f	$^1/_3$	$^2/_3$	0.1539(1)	0.2(1)	0.5
O1	6h	0.477(2)	−0.046(2)	0.25	1.5(3)	1
O2	12k	0.1695(6)	0.3390(6)	0.4068(6)	2.1(2)	1

[a] Space group $P6_3/mmc$, $a = 5.9246(2)$ Å, $c = 14.6761(5)$ Å. Reliability factors: $R_p = 6.1$, $R_{wp} = 7.9$, $R_{exp} = 4.3$, $\chi^2 = 3.4$. Bond lengths (Å): Ba1−O1 = 2.972(8) (×6), Ba1−O2 = 2.885(7) (×6), Ba2−O2 = 3.321(8) (×3), Ba2−O2 = 2.965(2) (×6), Ba2−O1 = 2.917(7) (×3), Ca−O2 = 2.213(6) (×6), Ti/W−O1 = 2.040(7) (×3), Ti/W−O2 = 1.902(5) (×3). Bond valence sums: Ba1 = 2.12, Ba2 = 1.68, Ca = 3.08, Ti/W = 4.64.

structure, being isostructural with several known 1:2 M-site ordered 6H perovskites reported in the literature.[5,6,12] The refinement data reveal that Ti/W are disordered at the 4f sites while the Ca atom occupies the 2a site. Accordingly, the structure (Figure 5) consists of two face-sharing Ti/WO_6 octahedra that are connected to isolated CaO_6 octahedra through corners. While CaO_6 octahedra are nearly regular with six equal Ca−O bond lengths (2.213 Å), Ti/WO_6 octahedra are distorted with two sets of Ti/W−O distances (2.040 and 1.902 Å). The distortion is such that the metal atoms are pushed away from each other across the shared common face, a result that can be understood as arising from the electrostatic repulsion of highly charged Ti/W atoms. Also the distortion is a manifestation of the second-order Jahn−Teller effect of d^0 metal atoms in octahedrally coordinated metal oxides in general.[1,18]

Bond valence sums of $Ba_3CaTiWO_9$ (Table 2) show certain systematics: while the sum is nearly ideal for Ba1, Ba2 is underbonded, correspondingly Ca is overbonded, and Ti/W are slightly underbonded. These features can be understood in terms of the geometrical constraints of the structure, arising from accommodating a large CaO_6 octahedron to the smaller face-shared Ti/WO_6 octahedra; necessarily, the bonds in the latter are stretched, while the Ca−O bonds are compressed, resulting in the observed bond valence sums.

From the Goldschmidt tolerance factors, *t* (Table 1), one would expect $Ba_3CaTiWO_9$ ($t = 0.997$) to form with the 3C structure. However, the fact that this oxide forms in a nearly ideal 1:2 M-site ordered 6H perovskite structure suggests that *t* alone is not the governing factor for the structures of the $Ba_3M^{II}M^{IV}WO_9$ series.

For the other $Ba_3M^{II}TiWO_9$ oxides containing divalent atoms Mg, Co, Ni, and Zn, while the major phase is the 6H perovskite oxide that is similar to $Ba_3CaTiWO_9$, we invariably see two minor impurities, $BaWO_4$ and a 1:1 M-site ordered 3C double perovskite oxide that is similar to Ba_2MgWO_6.[19] While the formation of $BaWO_4$ could be understood as arising from the strong affinity of the basic BaO to the highly acidic WO_3, the occurrence of 3C double perovskite impurity provides insight into the actual mechanism of phase formation in these systems. Considering that we see a large proportion of the 3C phase in the early stages of synthesis at lower temperatures (≤1200 °C) that progressively decreases at higher temperature (albeit $BaWO_4$ persists), we believe that a 3C double perovskite forms first and transforms at higher temperatures to the 6H phase. Indeed, we could prepare the intermediate 3C phase in the

(18) Bhuvanesh, N. S. P.; Gopalakrishnan, J. *J. Mater. Chem.* **1997**, *7*, 2297.
(19) Filip'ev, V. S.; Shatalova, G. E.; Fesenko, E. G. *Kristallografiya* **1974**, *19*, 386.

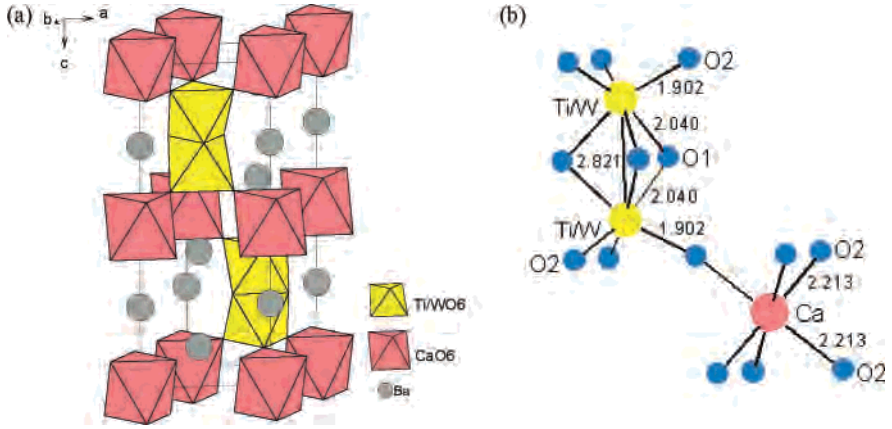

Figure 5. (a) Crystal structure of $Ba_3CaTiWO_9$ (6H). (b) Coordination geometry around Ti/W and Ca atoms in the structure. The bond lengths (Å) are also given.

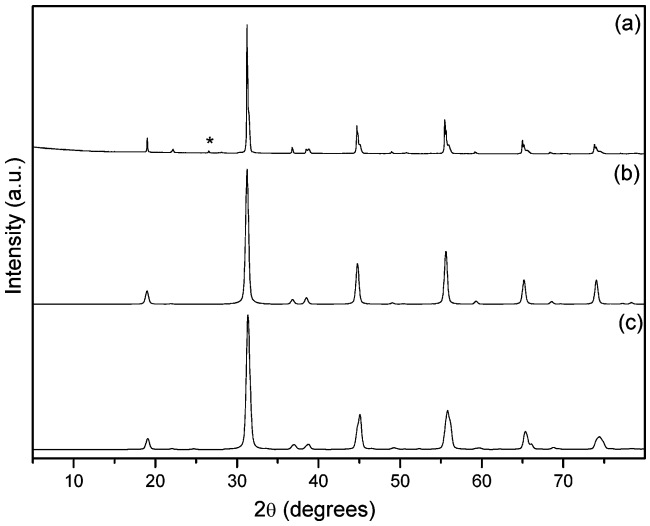

Figure 6. Powder XRD pattern of (a) $Ba_3ZnTiWO_9$ (3C). Simulated patterns of part a based on Ba_2ZnWO_6 (b) and Sr_2CoWO_6 structures (c) are shown. The impurity phase reflection of $BaWO_4$ (asterisk) is marked.

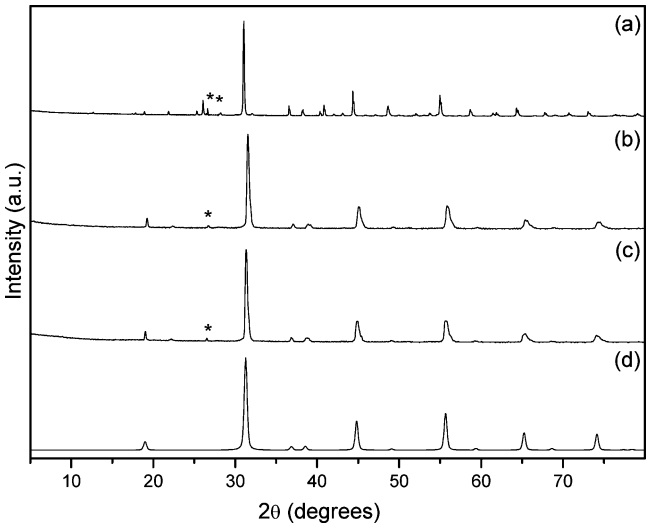

Figure 7. Powder XRD patterns: (a) $Ba_3ZnTiWO_9$ (6H); (b) $Ba_{2.35}Sr_{0.65}ZnTiWO_9$; (c) $Ba_{2.36}Sr_{0.64}ZnTiWO_9$. In part d, the simulated pattern of part c based on Ba_2ZnWO_6 is shown. Impurity phase reflections of $BaWO_4$ (asterisks) are marked.

$Ba_3ZnTiWO_9$ system by careful control of synthesis conditions (Table 1). While the powder XRD pattern of the 3C $Ba_3ZnTiWO_9$ system (Figure 6a) is by and large similar to that of a 1:1 ordered 3C double perovskite like Ba_2ZnWO_6 (Figure 6b) with the cation distribution $Ba_2(Zn_{2/3}Ti_{1/3})(W_{2/3}Ti_{1/3})O_6$, the distortion and asymmetry of several reflections in the XRD pattern suggest a lower symmetry structure most likely arising from the random occupancy of $^1/_3$Zn (4b) and $^1/_3$W (4a) sites by Ti in the Ba_2ZnWO_6 structure. The powder XRD pattern could be better modeled on the basis of the monoclinic $P2_1/n$ Sr_2CoWO_6 structure,[20] where Ba replaces Sr, $Zn_{2/3}Ti_{1/3}$ occupies the Co position (2c), and $W_{2/3}Ti_{1/3}$ occupies the W position (2d). Presumably, the distortion to low symmetry arises from a size mismatch between ZnO_6 and WO_6 octahedra.

The 3C $Ba_3ZnTiWO_9$ system transforms completely to the 6H structure at higher temperatures (1300 °C; Figure 7a), indicating that the 6H structure is the stable structure for all of the $Ba_3M^{II}TiWO_9$ phases investigated. The 3C → 6H transformation at high temperatures is consistent with the generally observed H → C transformation of perovskite oxides under pressure:[21] while pressure tends to decrease the tolerance factor (t) for perovskite (AMO_3) compositions (arising from a larger compressibility of A−O bonds than of M−O bonds), temperature would have the opposite effect.

In an effort to further probe the role of t on the stabilization of 3C versus 6H structures for $Ba_3M^{II}TiWO_9$ oxides, we investigated the substitution of Sr for Ba in $Ba_3ZnTiWO_9$. We prepared two compositions in the system $Ba_{3-x}Sr_xZnTiWO_9$ for x = 0.64 and 0.65; these compositions are tailored such that their t values (1.027 and 1.026) closely match the t value for $Ba_3ZnTa_2O_9$ (t = 1.027). We find that both of the compositions are formed with the 1:1 M-site ordered 3C structure (Figure 7) and retain the same structure even upon prolonged heating at 1300 °C, conditions under which $Ba_3ZnTiWO_9$ transforms to the 6H structure. The result clearly reveals the role of t for stabilization of 6H versus 3C structures: a lower t favors the 3C

(20) Viola, M. C.; Martinez-Lope, M. J.; Alonso, J. A.; Martinez, J. L.; De Paoli, J. M.; Pagola, S.; Pedregosa, J. C.; Fernandez-Diaz, M. T.; Carbonio, R. E. *Chem. Mater.* **2003**, *15*, 1655. Zhou, Q.; Kennedy, B. J.; Elcombe, M. M. *J. Solid State Chem.* **2007**, *180*, 541.

(21) For example, see: Goodenough, J. B. *Rep. Prog. Phys.* **2004**, *67*, 1920.

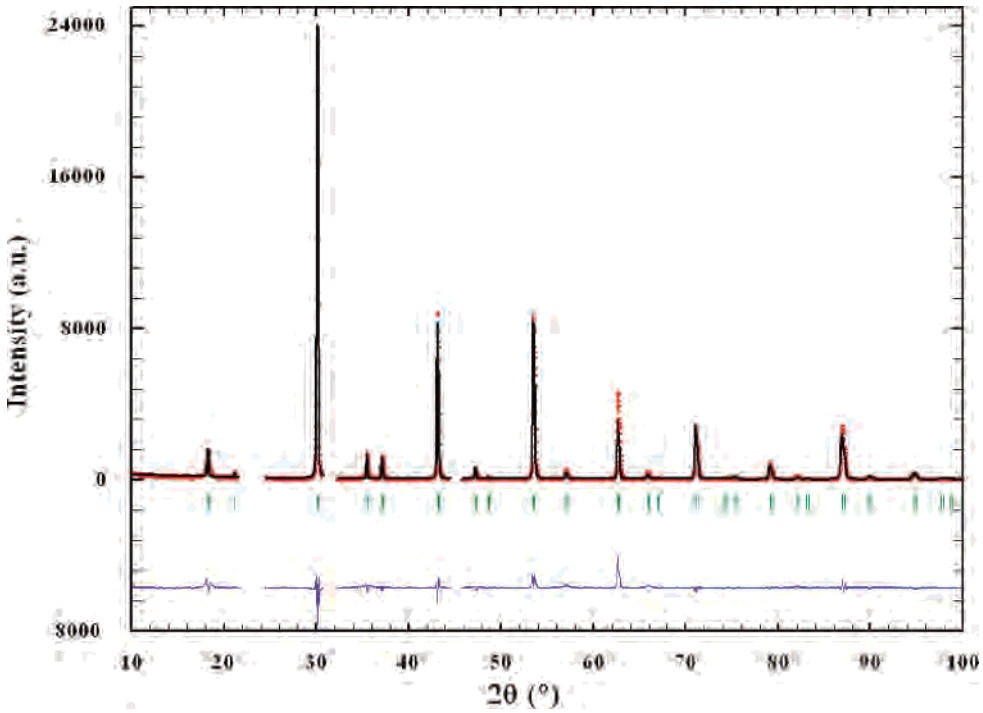

Figure 8. Rietveld refinement of the structure of $Ba_3CaZrWO_9$ (3C) from powder XRD data. Observed (●), calculated (—), and difference (bottom) profiles are shown. The vertical bars indicate positions of the Bragg reflections. The 2θ regions (21.80−24.45, 30.97−32.25, and 44.70−45.75°) corresponding to $CaZrO_3$ impurity reflections are excluded from the refinement.

structure, while a higher *t* favors the 6H structure. It must, however, be pointed out that this conclusion appears to hold only for a given series of perovskite oxides, such as $Ba_{3-x}Sr_xZn^{II}TiWO_9$; it may not be applicable, in general, to all of the $Ba_3M^{II}M^{IV}WO_9$ compositions. Thus, a composition such as $Ba_3CaTiWO_9$, which has the smallest *t* (0.997) among the $Ba_3M^{II}TiWO_9$ system, adopts the 6H structure, although one would have expected a 3C structure on the basis of the *t* factor alone. The results indeed reveal the complexity of bonding and crystal-chemical (size) considerations that underlie the stability of 3C versus 6H structures for the $Ba_3M^{II}TiWO_9$ oxides.

We investigated the formation of $Ba_3M^{II}ZrWO_9$ oxides in an effort to probe the role of Ti^{IV} versus Zr^{IV} on the perovskite structures. While we could not prepare single-phase materials of this composition by the ceramic route, we could prepare $Ba_3CaZrWO_9$ as a single phase by an indirect metathesis route involving the reaction of $BaCl_2$, $CaCO_3$, ZrO_2, and WO_3, together with Li_2CO_3. Product formation occurs according to the metathesis reaction (1). After washing and drying, the powder XRD pattern of the product (Figure 3e) showed it to be a single-phase $Ba_3CaZrWO_9$ perovskite with the 3C structure (but for a small impurity of $CaZrO_3$). A refinement of its structure from powder XRD data (Figure 8 and Table 3) confirmed the 1:1 ordered 3C structure for $Ba_3CaZrWO_9$ with the distribution of cations, $Ba_2(Ca_{2/3}Zr_{1/3})(W_{2/3}Zr_{1/3})O_6$ at the M sites (4b and 4a; Figure 9). Upon heating at high temperatures, the phase does not transform to the 6H structure; instead, it decomposes to a multiphasic mixture. Presumably, a smaller tolerance factor ($t = 0.979$) arising from the larger radius of Zr^{IV} and the inability of the latter to support a strong anion polarization

Table 3. Crystallographic Data for $Ba_3CaZrWO_9$ (3C) Perovskite, Together with Selected Bond Lengths and Bond Valence Sums[a]

atom	site	*x*	*y*	*z*	*B* (Å^2)	occupancy
Ba	8c	0.25	0.25	0.25	0.08(4)	1.0
Ca1	4a	0.0	0.0	0.0	0.10	0.67
Zr1	4a	0.0	0.0	0.0	0.10	0.33
W2	4b	0.5	0.5	0.5	0.05	0.67
Zr2	4b	0.5	0.5	0.5	0.05	0.33
O	24e	0.265	0.0	0.0	0.4(1)	1.0

[a] Space group $Fm\bar{3}m$, $a = 8.3801(1)$ Å. Reliability factors: $R_p = 12.6$, $R_{wp} = 17.6$, $R_{exp} = 6.28$, $\chi^2 = 7.86$. Bond lengths (Å): Ba−O = 2.965 (×12), Ca1/Zr1−O = 2.221 (×6), W2/Zr2−O = 1.969 (×6). Bond valence sums: Ba = 1.91, Ca1/Zr1 = 2.92, W2/Zr2 = 5.27.

(Zr−O bonds are more ionic than Ti−O bonds) render the 6H structure inaccessible for $Ba_3CaZrWO_9$.

Blasse[13] in his seminal work on perovskite oxides has discussed the factors that govern the stabilization of 3C versus 6H perovskite structures for $A_2MM'O_6$ and $A_3MM'_2O_9$. While it was generally believed that cation−cation bonding (the presence of d electrons on M and M′ atoms) favors the 6H structure, Blasse pointed out that this is not the real reason for the formation of H structures. He emphasized that anion polarization is an important factor that favors H structures. Stabilization of the 6H structure over the 3C structure for the $Ba_3M^{II}TiWO_9$ series is consistent with Blasse's ideas. Thus, the 6H structure, which allows a greater polarization of anions [manifest in the form of a strong distortion of Ti/WO_6 octahedra that are face-shared (Figure 5)] than the 3C structure, is favored for the $Ba_3M^{II}TiWO_9$ oxides. In other words, the 6H structure seems to be favored for the Ti/W pair because they can be displaced from the center of symmetry of their octahedral site by a ferroic displacement. This is not the case for the larger Ta^V

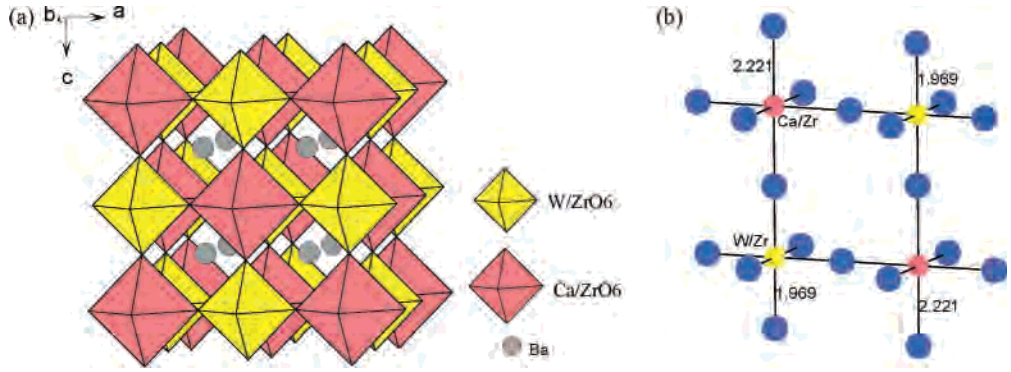

Figure 9. (a) Crystal structure of $Ba_3CaZrWO_9$ (3C). (b) Coordination geometry around W/Zr and Ca/Zr in the structure. The bond lengths (Å) are also given.

and Zr^{IV} ions, which makes the electrostatic repulsion across the shared common face prohibitive for Ta−Ta and Zr−W interactions, rendering the 6H structure inaccessible for $Ba_3MM'_2O_9$ compositions containing these ions.

Finally, it must be mentioned that we could not prepare a 1:2 ordered $Ba_3M^{II}TiWO_9$ perovskite oxide with a 3C structure similar to $Ba_3ZnTa_2O_9$. Even prolonged annealing of $Ba_{3-x}Sr_xZnTiWO_9$ phases that are stabilized in the 1:1 3C structure does not order them into the $Ba_3ZnTa_2O_9$ structure. It seems that 1:2 ordering of three different octahedral site M atoms in the 3C perovskite structure (which would necessarily involve an ordering of Ti and W at the Ta sites of the $Ba_3ZnTa_2O_9$ structure) is much more difficult than the ordering of only two M atoms, viz., Zn and Ta, in the 3C structure.

Conclusions

In summary, our investigations of $Ba_3M^{II}M^{IV}WO_9$ oxides have shown that the 6H perovskite structure (hexagonal, $P6_3/mmc$) is stable at ≥1300 °C for M^{IV} = Ti and M^{II} = Ca, Zn, Mg, Co, and Ni. For M^{II} = Zn, an intermediate 3C phase was obtained at lower temperatures (1200 °C), which transforms to the 6H structures at higher temperatures, revealing the possible mechanism of the formation of phases in general: first, a partially ordered 3C double perovskite, $Ba_2(M^{II}_{2/3}Ti^{IV}_{1/3})(W_{2/3}Ti^{IV}_{1/3})O_6$, is formed, which converts to the fully ordered 6H structure at higher temperatures. Partial substitution of Sr[22] for Ba in the members, $Ba_{3-x}Sr_xZnTiWO_9$, stabilizes the 3C structure instead of the 6H structure. Although we have not been able to prepare a 1:2 ordered 3C perovskite $Ba_3M^{II}TiWO_9$ similar to $Ba_3ZnTa_2O_9$, the 6H phases of the $Ba_3M^{II}TiWO_9$ series could themselves be useful dielectric ceramics, as shown by the recent investigations of Khalyavin et al.[23] on the 6H Ba_3MTiWO_9 (M = Mg, Zn) systems.

Acknowledgment. We thank the Department of Science and Technology (DST), Government of India, for support of this research. We also thank CSIR, New Delhi, India, for grants of a research project (J.G.) and a fellowship (R.M.). J.G. thanks the DST for the award of a Ramanna Fellowship.

Supporting Information Available: Indexed powder XRD data for 3C and 6H $Ba_3ZnTiWO_9$ and 3C $Ba_{2.36}Sr_{0.64}ZnTiWO_9$. This material is available free of charge via the Internet at http://pubs.acs.org.

IC7007655

(22) Shannon, R. D. *Acta Crystallogr., Sect. A* **1976**, *32*, 751.
(23) Khalyavin, D. D.; Senos, A. M. R.; Mantas, P. Q. *Mater. Res. Bull.***2007**, *42*, 126.